M. KUKURYK*,♯

ANALYSIS OF DEFORMATION AND MICROSTRUCTURAL EVOLUTION IN THE HOT FORGING OF THE Ti-6Al-4V ALLOY

ANALIZA ODKSZTAŁCENIA I PROGNOZOWANIA MIKROSTRUKTURY W PROCESIE KUCIA STOPU Ti-6Al-4V NA GORĄCO

The paper presents the analysis of the three-dimensional strain state for the cogging process of the Ti-6Al-4V alloy using the finite element method, assuming the rigid-plastic model of the deformed body. It reports the results of simulation studies on the metal flow pattern and thermal phenomena occurring in the hot cogging process conducted on three tool types. The computation results enable the determination of the distribution of effective strain, effective stress, mean stress and temperature within the volume of the blank. This solution has been complemented by adding the model of microstructure evolution during the cogging process. The numerical analysis was made using the DEFORM-3D consisting of a mechanical, a thermal and a microstructural parts. The comparison of the theoretical study and experimental test results indicates a potential for the developed model to be employed for predicting deformations and microstructure parameters.

Keywords: hot forging, titanium alloy, finite element method, microstructure evolution

W pracy przedstawiono analizę przestrzennego stanu odkształcenia dla procesu kucia wydłużającego stopu tytanu Ti-6Al-4V z wykorzystaniem metody elementów skończonych z założeniem sztywnoplastycznego modelu odkształcanego ciała. Przedstawiono wyniki prac związanych z symulacją schematu płynięcia metalu i zjawisk cieplnych w procesie kucia na gorąco w trzech rodzajach narzędzi kuźniczych. Rezultaty obliczeń umożliwiają określenie rozkładu intensywności odkształcenia, intensywności naprężeń, naprężeń średnich i temperatury w objętości odkuwki. Rozwiązanie uzupełniono o model rozwoju mikrostruktury podczas kucia. Analizę numeryczną wykonano z wykorzystaniem programu DEFORM-3D, składającego się z części mechanicznej, termicznej i mikrostrukturalnej. Porównanie teoretycznych i eksperymentalnych rezultatów badań wskazuje na możliwość zastosowania opracowanego modelu do prognozowania odkształceń i parametrów mikrostruktury.

1. Introduction

A majority of high-strength constructional elements of titanium alloys are manufactured by hot plastic working methods, chiefly by open die forging or die forging. Most often, $\alpha + \beta$ two-phase titanium alloys are used, which are characterized by high relative strength, good high-temperature creep resistance (up to 450°C), high fatigue strength under corrosive conditions, corrosion resistance in many media and good weldability [1]. A determining influence on the mechanical and service properties of a product is exerted by temperature, the method, nature and magnitude of deformation and the heat treatment of the blank [2].

The great non-uniformity of deformations in the forging process makes the production of internal-quality titanium forgings much more difficult compared to imparting the proper shape and geometry to the forgings [3]. In order to maintain a relatively small gradient of properties within the entire volume of the blank and, at the same time, their required level, cogging forging is used in anvils with a purpose-designed shape [4]. In the hot plastic working of titanium alloys, many factors are involved, which make the obtaining of products

with the required microstructure and properties difficult and sometimes even impossible; these include: high affinity of titanium to oxygen, their low thermal conductivity and high heat capacity, which lead to the localization of heat during stock deformation and significant dependence of plastic flow resistance on the strain rate [5].

During deformation, micro-regions occur in the blanks, which differ in the value of temperature due to the physical properties and the features of the allotropic change $Ti_\alpha \leftrightarrow Ti_\beta$ and the deformation conditions. The determination of temperature distribution within the deformation zone during the titanium alloy forging process is important because of the effect of temperature on the properties and structure of the material being deformed [6, 7]. Hence, by controlling the thermomechanical state of the deformation zone in the forging process it will be possible to substantially influence the mechanical and service properties of the products [8].

The cogging forging process consists of many partial, interrelated reductions done in a specific order. Assuming the cyclical nature and repeatability of the phenomena, the study of the stress and strain state can be reduced to the examination of one engineering pass (two consecutive reductions with

* CZESTOCHOWA UNIVERSITY OF TECHNOLOGY, FACULTY OF MECHANICAL ENGINEERING AND COMPUTER SCIENCE, 42-200 CZĘSTOCHOWA, AL. ARMII KRAJOWEJ 21, POLAND
♯ Corresponding author: kukuryk@iop.pcz.pl

the simultaneous rotation of the material by 90°), which will considerably simplify the forging process.

A finite element method-based model has been developed within the present work, which enables the prediction of the distribution of deformation parameters (strain, stress, temperature) and microstructure evolution during the cogging process of the Ti-6Al-4V alloy in forging anvils of three types. Special emphasis is placed on the correct determination of the mechanical and thermal properties of the examined material under hot forging conditions. The positive results of numerical studies and their experimental verification allow the practical application of computer modeling to develop the rational shapes of forging tools and determine the optimal parameters of the cogging process. This operation will result in an improvement in the quality of blanks made of two-phase titanium alloys, with the capability to predict the microstructure parameters.

2. Thermo-mechanical model

A three-dimensional rigid-plastic finite element method was used in the simulation of metal flow and heat transfer during the process of forging of the Ti-6Al-4V alloy. For the analysis of the forging process, DEFORM 3D, a commercial software program developed by Battel Columbus Lab. of the USA, was employed. The DEFORM 3D program, with coupled thermo-mechanical and microstructural evolution, relies on the finite element method [9]. The numerical computation enabled the assessment of the effective strain, effective stress and temperature distributions in the deformed material in three types of anvils.

The basic equations that are to be satisfied are: the equilibrium equation, the incompressibility condition and the constitutive relationship. The solution of the original boundary-value problem is obtained by solving the dual variational problem, where the first-order variation of the functional vanishes:

$$\delta \varphi = \int_V \bar{\sigma} \delta \dot{\bar{\varepsilon}} \, dV + \int_V K \dot{\varepsilon}_v \delta \dot{\varepsilon}_v \, dV - \int_{S_F} F_i \delta v_i \, dS = 0 \quad (1)$$

where $\bar{\sigma}$ is the effective stress, $\dot{\bar{\varepsilon}}$ is the effective strain rate, $\dot{\varepsilon}_v$ is the volumetric strain rate, V and S are, respectively, the volume and the surface area of the material, F_i is the force on the boundary surface of S_F, K the penalty constant, δv_i is the arbitrary variation, $\delta \dot{\bar{\varepsilon}}$ and $\delta \dot{\varepsilon}_v$ are the variations in strain-rate derived from δv_i. Eq. (1) can be converted to non-linear algebraic equations by using the procedure of finite element discretization. The solution of the non-linear simultaneous equations is obtained by the Newton-Raphson method. The flow stress (σ) is a function of strain (ε), strain rate ($\dot{\varepsilon}$) and temperature (T) (Fig. 1, experimental results):

$$\sigma = f(\varepsilon, \dot{\varepsilon}, T) \quad (2)$$

The flow curves of the model as per Eq. (2) are consistent with the experimental data in the temperature range of 1073-1273 K, the true strain range of 0.105 - 0.693 and the strain rate range of 1.0 - 5.5 s^{-1}. The flow stress of the

Ti-6Al-4V alloy obtained from compression tests is input to the FEM simulation system. The computer program uses an interpolation mechanism that allows the values of stress and strain rates to be chosen from the database.
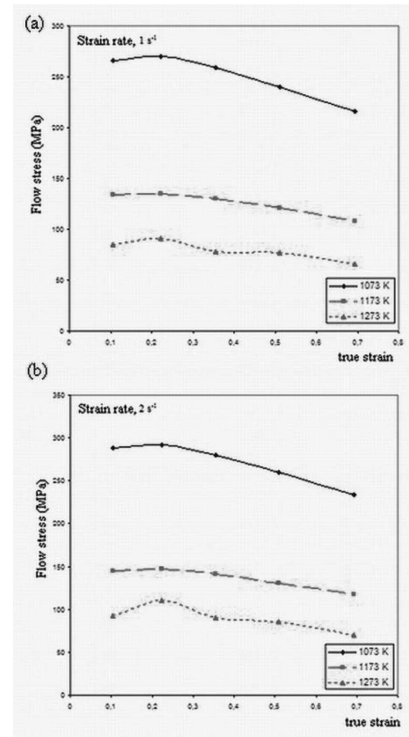

Fig. 1. Variation of flow stress for the Ti-6Al-4V alloy as a function of true plastic strain and temperature, for different strain rate values, i.e.: (a) $- \dot{\varepsilon} = 1 s^{-1}$ and (b) $- \dot{\varepsilon} = 2 s^{-1}$

The distribution of workpiece and die temperatures can be obtained by solving the energy balance equation, expressed by

$$\nabla^T \cdot (k \nabla T) + q = \rho c_p \frac{\partial T}{\partial t} \quad (3)$$

where k is the thermal conductivity, T is temperature, q is the rate of heat generated due to plastic deformation, ρ is density, c_p is the specific heat and t is time. The first term and the third term represent the heat transfer rate and the internal heat generation rate, respectively.

Along the boundaries of the deforming material, either temperature, T is prescribed on the part with surface S_T, or the heat flux q_n is prescribed on the remainder of surface S_q. The energy balance equation, Eq. (3) is written in a weak form as follows:

$$\int_V k T_{,i} \delta T_{,i} \, dV + \int_V \rho c_p \dot{T} \delta T \, dV - \int_V \alpha (\bar{\sigma} \dot{\bar{\varepsilon}}) \delta T \, dV - \int_{S_q} q_n \delta T \, dS = 0 \quad (4)$$

where $q_n = k T_{,n} = k T_{,i} n_i$ is the boundary heat flux, α is the fraction of deformation energy that converts into heat, and was assumed to be 0.9.

The effect of friction at the workpiece–tooling interfaces was allowed for with the following equation:

$$f = -m \tau_p \left[\frac{2}{\pi} \tan^{-1} \left(\frac{|v_r|}{a} \right) \right] \frac{v_r}{|v_r|} \quad (5)$$

where v_r is the relative velocity, a – a small constant ($a = 0.0001$), m – the friction factor ($0 \leqslant m \leqslant 1$) and τ_p the local flow stress in shear.

3. Microstructural evolution

3.1. Dynamic recrystallization (DRX)

In the hot cogging process, microstructure change takes place easily through the deformation of the material. The microstructure change occurring due to deformation is generally called dynamic recrystallization. The theoretical-experimental relationships implemented in the DEFORM 3D program environment were used for deriving the equations of the microstructure evolution model. The evolution of the microstructure during the cogging process is dependent on the dynamic recrystallization and grain growth process that is determined by the time of holding the material at high temperature. This mechanism occurs during deformation when the strain exceeds a critical strain value [10]. Experimental data must be collected under various strain, strain rate and temperature conditions. The dynamic recrystallization is a function of strain, strain rate, temperature and initial grain size, which change in time. It is very difficult to model dynamic recrystallization concurrently during forming [11]. Instead, the dynamic recrystallization is computed in the step that follows immediately after the deformation stops. The critical strain ε_c is usually a fraction of the strain ε_p at which the flow stress reaches its maximum:

$$\varepsilon_c = a_2 \, \varepsilon_p \tag{6}$$

where ε_p denotes the strain corresponding to the flow stress maximum. The value of ε_p is determined experimentally and is usually a function of strain rate, temperature, and initial grain size:

$$\varepsilon_p = a_1 \, d_0^{n_1} \, \dot{\bar{\varepsilon}}^{m_1} \exp \frac{Q_1}{RT} + c_1 \tag{7}$$

The Avrami equation is used to describe the relationship between DRX volume fraction and the effective strain:

$$X_{DRX} = 1 - \exp \left[-\beta_d \left(\frac{\bar{\varepsilon} - a_{10}\varepsilon_p}{\varepsilon_{0.5}} \right)^{k_d} \right] \tag{8}$$

in which $\varepsilon_{0.5}$ denotes the strain for 50% recrystallization:

$$\varepsilon_{0,5} = a_5 \, d_0^{n_5} \, \dot{\bar{\varepsilon}}^{m_5} \exp \frac{Q_5}{RT} + c_5 \tag{9}$$

The recrystallized grain size is expressed as a function of initial grain size, strain, strain rate and temperature:

$$d_{DRX} = a_8 \, d_0^{h_8} \, \bar{\varepsilon}^{n_8} \, \dot{\bar{\varepsilon}}^{m_8} \exp \frac{Q_8}{RT} + c_8 \tag{10}$$

where if $d_{DRX} \geqslant d_0$ then $d_{DRX} = d_0$

3.2. Grain growth

Grain-growth modeling is performed for the material in a strain-free state, i.e., before hot working or after the recrystallization has been completed. For this purpose, the classical phenomenological grain growth relationship is employed. The kinetics is described by the following equation:

$$d_{gg} = \left[d_{ave}^{m_9} + a_9 \, t \, \exp \left(-\frac{Q_9}{RT} \right) \right]^{\frac{1}{m_9}} \tag{11}$$

where d_{gg} denotes the average grain size after the growth, a_9 and m_9 are material constants and Q_9 is the activation energy.

3.3. Average grain size

The mixture law was employed to calculate the recrystallized grain size for incomplete recrystallization:

$$d_{ave} = X_i \, d_{ave, i} + (1 - X_i) \, d_{ave, i-1} \tag{12}$$

where $d_{ave, i-1}$ is the average grain size for the previous step, X_i – the recrystallization volume fraction and $d_{ave, i}$ – the average grain size for the current step.

The nomenclature of the above formulation is as follows: T – temperature (K); X_{DRX} – the volume fraction of dynamic recrystallization; $\bar{\varepsilon}$ – effective strain; $\varepsilon_{0.5}$ – strain for 50% recrystallization; $\dot{\bar{\varepsilon}}$ – effective strain rate (s^{-1}); $t_{0.5}$ – time for 50% recrystallization (s); ε_c – critical strain (the strain above which dynamic recrystallization occurs); R – gas constant (8,314472 J/(K mol)); t – time (s); d_0 – initial grain size (μm); d_{ave} – average grain size (μm); ε_p – peak strain (strain at the peak value of effective stress); a_{1-10} – material data (experimental coefficients); h_{1-8}, n_{1-8}, m_{1-9} – material data (experimental coefficients); Q_{1-9} – material data (activation energies); β_d – material data (an experimental coefficient); k_d – material data (the experimental exponent).

4. Results and discussion

The flow stress values for the Ti-6Al-4V alloy were taken based on plastometric tests carried out for different values of strain and strain rates, and for a fixed range of hot plastic working temperature ($\sigma = f(\varepsilon, \dot{\varepsilon}, T)$). The tests included the compression of ø30x30mm axially symmetrical specimens on a cam plastometer, type MAEKAWA – Japan, with the specimens having the following chemical composition: Ti – the matrix, Al – 6.10%, V – 4.20%, Fe – 0.15%, C – 0.01%, H – 0.016%, N – 0.06% and O – 0.12%. The specimens were deformed at temperatures of 1073K – 1273K and at strain rates of 0.5 – 5.5 s^{-1}. The specimens were heated up to the deformation temperature in an automatically controlled electric furnace. The total deformation, as calculated from the specimen height change, was 0.105 – 0.693. The obtained results allowed the determination of the flow stress values, as dependent on the actual strain, strain rate and temperature, which were input to the program with the aim of evaluating the best rheological model for the material being deformed.

Example relationships of flow stress during upset forging of Ti-6Al-4V alloy specimens versus temperature for two selected strain rates, i.e. 1.0 s^{-1} and 2.0 s^{-1}, and for three temperature values (1073K, 1173K and 1273K), are shown in Figure 1. The determined curves of $\sigma = f(\varepsilon)$ exhibit a characteristic flow stress maximum that occurs at a strain value slightly higher than $\varepsilon = 0.2$. The determined flow curves allowed for the effects associated with strain localization and temperature increment due to the conversion of work into heat.

In numerical computations and in experimental tests, ø80 mm-diameter and 200 mm-long stock of the Ti-6Al-4V alloy was taken. For the titanium alloy under examination and for the anvil material X37CrMoV51, the thermal characteristics, such as density, specific heat and thermal conductivity, were assumed based on experimental data and were input as functions of temperature. The initial anvil temperature was taken as 300°C, i.e. the anvil heating temperature in industrial conditions. Forging was carried out in two consecutive reductions with tilting the workpiece by an angle of 90°, while retaining a constant value of true reduction of $\varepsilon_h = 0.35$ and a constant relative feed of $l_w = 0.75$. The cogging process was conducted in flat anvils, radial-rhombic anvils with an impression angle of 135°/135°, and special tri-radial anvils, as shown in Figure 2.
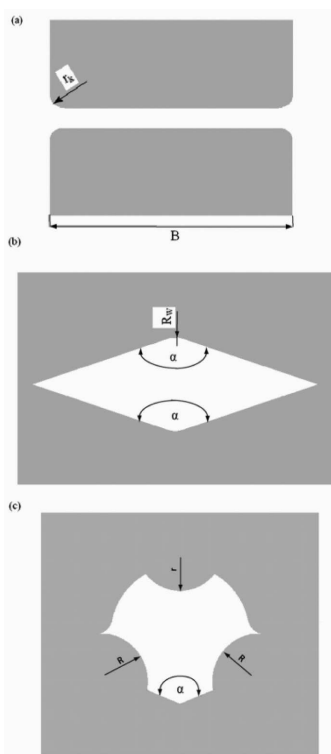
Fig. 2. Shape of anvils: (a) – flat ($r_k = 0.10B$), (b) – radial-rhombic with an impression angle of $\alpha = 135°/ 135°$ ($R_w = 0.35D_0$), (c) – special tri-radial ($R/D_0 = 0.40$, $r/D_0 = 0.35$ and $\alpha = 135°$)

Some more important values of the determined coefficients occurring in formulas (6)-(12) are as follows:

$a_1 = 0.005$, $a_2 = 0.83$, $n_1 = 0.40$, $m_1 = 0.017$, $c_1 = 0.35$, $Q_1 = 41700$, $\beta_d = 0.6903$, $a_5 = 0.0011$, $h_5 = 0.25$, $m_5 = 0.05$, $Q_5 = 24430$, $a_8 = 1600$, $h_8 = 0.70$, $n_8 = 0.80$, $Q_8 = -52235$, $m_8 = -0.33$, $c_8 = 0.80$.

The relationship of density versus temperature for the Ti-6Al-4V alloy is expressed below:

$$\rho = -2 \cdot 10^{-14}T^5 + 3 \cdot 10^{-11}T^4 - 4 \cdot 10^{-9}T^3 - \\ -3 \cdot 10^{-5}T^2 - 0.1211\,T + 4422.4 \tag{13}$$

The relationship between thermal conductivity for the Ti-6Al-4V alloy and temperature is expressed as follows:

$$\lambda = -7e^{-5}T^5 + 0.0031T^4 - 0.0524T^3 + 0.3761T^2 - 0.4206T + 6.6121 \tag{14}$$

The relationship between specific heat for the Ti-6Al-4V alloy and temperature is expressed as:

$$c_p = -0.0002T^5 + 0.0038T^4 - 0.0287T^3 + 0.1089T^2 - \\ -0.0877T + 2.3058 \tag{15}$$

The tests carried out enabled the determination of the local values describing the strain state, the stress state, the temperature distribution, and microstructural evolution during cogging of the Ti-6Al-4V alloy on flat dies and in selected shaped dies with the aim of developing the optimal forging system.

During cogging of a round cross-section material on flat anvils (Fig. 3a), the strain non-uniformity is relatively large. In the presented effective strain distribution after the second reduction ($\varepsilon_h = 0.70$), several characteristic zones can be distinguished. The region adjacent to the anvil surface undergoes deformation considerably less compared to the true reduction ($\bar{\varepsilon}/\varepsilon_h = 0.45 - 0.55$). The greatest strains occur in the central part of the blank ($\bar{\varepsilon}/\varepsilon_h = 1.04$); similarly, the side blank zones constitute a region of smaller strains ($\bar{\varepsilon}/\varepsilon_h = 0.45 - 0.55$). This part of the blank material is additionally subjected to the action of tensile stresses from the undeformed external zones and from the strongly deformed center (Fig. 3b).
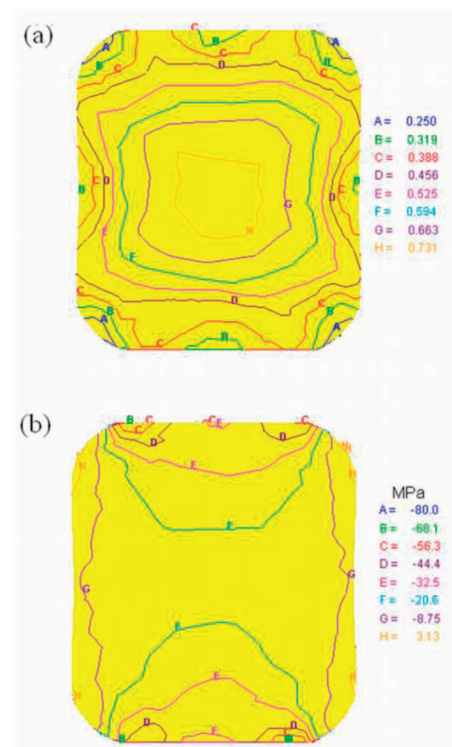

Fig. 3. Distribution of effective strain (a) and mean stress (b) on the specimen cross-sectional surface during cogging process in flat anvils after the second reduction ($\varepsilon_h = 0.70$)

Figure 4 represents the distribution of effective strain, mean stress, and temperature after the process of cogging of Ti-6Al-4V alloy specimens in radial-rhombic anvils with an

impression angle of 135°/135° after the second reduction (ε_h = 0.70). The anvils used in the tests showed a favorable effect on the strain and stress distribution in the process of forging of the titanium alloy under investigation. The greatest strains penetrate into the axial zone of the blank, where the maximum values of $\bar{\varepsilon}$ considerably exceed the preset strain value ($\bar{\varepsilon}/\varepsilon_h$ =1.77), which favorably influences it getting forged out. The side blank zones and areas under the anvil corner radii exhibit a set of smaller effective strain values of $\bar{\varepsilon}/\varepsilon_h$ = 0.68 - 0.86 (Fig. 4a).

The relatively large surface of contact between the deformed material and the tool is the cause of the advantageous state of stress in the central part of the blank. For the 135°/135° angle radial-rhomboid anvils, no tensile stresses were found to occur in the axial zone of the blank. The presented distribution of mean stress (Fig. 4b) indicates a possibility of tensile stresses occurring only in a very small area in the side zones of the blank.

During forging, considerable thermal instability was found in the internal blank zones, being dependent on the local values of plastic deformation work and friction forces work (Fig. 4c). Furthermore, a stable temperature distribution was observed in the middle part of the blank. It was caused by the release of plastic deformation heat. The contact of the hot metal with the cool tool resulted in considerable temperature gradients on the contact surfaces ($\Delta T = 80 - 130°C$). Measurements of the surface temperature of the blank after deformation using a thermovision camera showed an agreement between this temperature and the computed temperature (with differences of ±10°C).
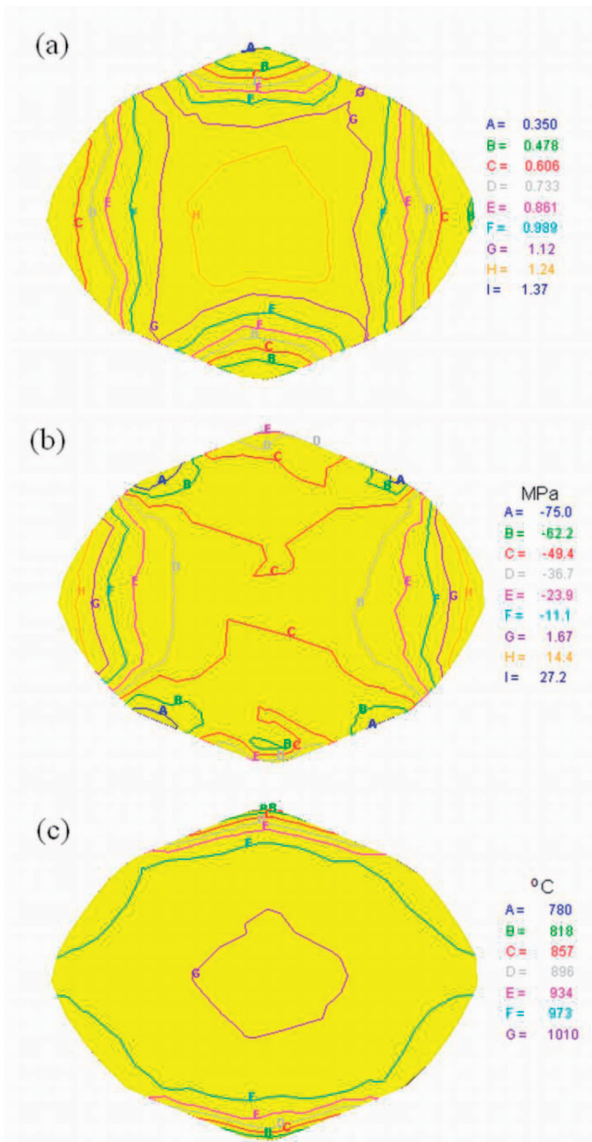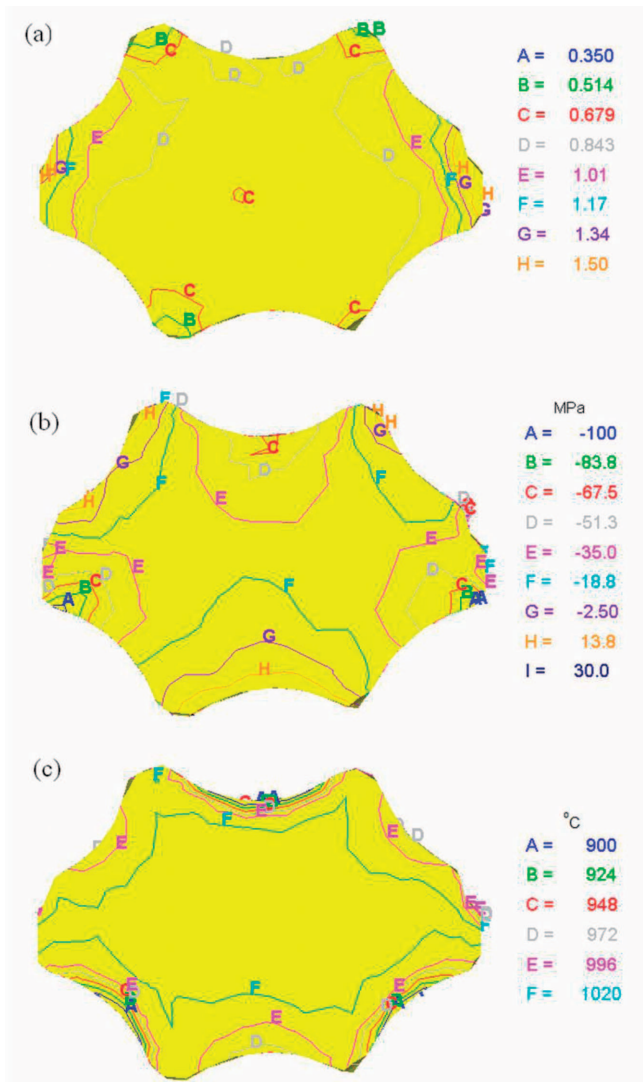

Fig. 4. Distribution of effective strain (a), mean stress (b) and temperature (c) on the specimen cross-sectional surface after cogging process in radial-rhombic anvils with an impression angle of α =135°/135°. True strain ε_h = 0.70

Fig. 5. Distribution of effective strain (a), mean stress (b) and temperature (c) on the specimen cross-sectional surface after cogging process in special tri-radial anvils. True strain ε_h = 0.70

Figure 5 represents the distribution of effective strain, mean stress, and temperature after the cogging of Ti-6Al-4V alloy specimens in special tri-radial anvils after the second reduction (ε_h = 0.70). The shaped anvils used in the tests showed a favorable effect on the strain and stress distribution in the Ti-6Al-4V alloy forging process (Fig. 5a). The greatest effective strain values occurred in the blank areas situated under the convex anvil surfaces ($\bar{\varepsilon}/\varepsilon_h$ =1.20 - 1.44). The middle part of the blank represented the region of the smallest effec-

tive strain values ($\bar{\varepsilon}/\varepsilon_h = 0.97$). A great advantage of forging in these anvils is a relatively high uniformity of effective strain distribution ($\bar{\varepsilon}/\varepsilon_h = 0.97 - 1.44$). The large surface of contact between the deformed material and the tool was the cause of the favorable stress state in the central part of the blank deformed in the special tri-radial anvils (Fig. 5b). The contact of the hot metal and the cool tool resulted in considerable temperature gradients in the vicinity of the contacting surfaces ($\Delta T = 50 - 100°C$, Fig. 5c).
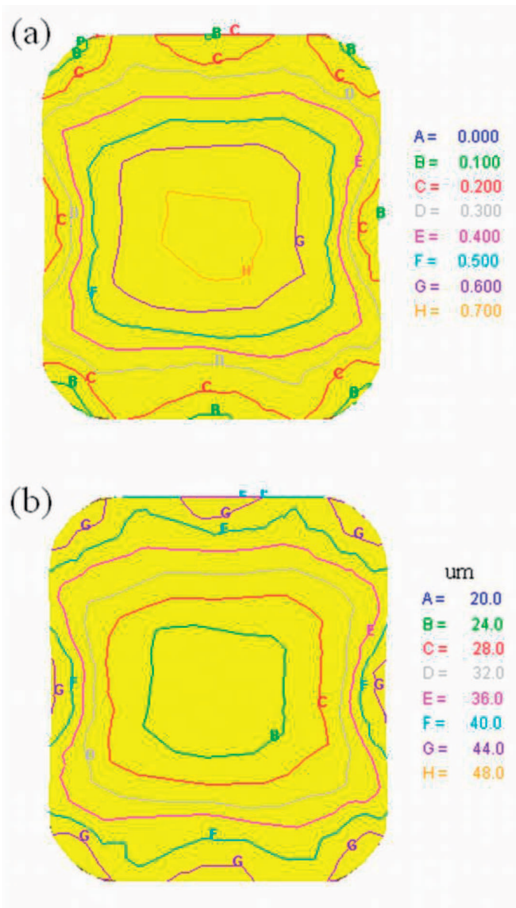

Fig. 6. Distribution of the dynamically recrystallized volume fraction (a) and mean grain size (b) on the specimen cross-sectional surface after cogging process in flat anvils. True strain $\varepsilon_h = 0.70$

The distribution of the dynamically recrystallized volume fraction and the distribution of mean grain size on the cross-sectional surface of Ti-6Al-4V alloy specimens after the cogging (after the second reduction) in flat anvils are shown in Figure 6. The microstructure examination showed that the process of deformation in flat anvils proceeds non-uniformly across the specimen cross-section, which results in an inhomogeneity of the microstructure in the form of the presence of zones with a different degree of recrystallization and a varying mean grain size. Dynamic recrystallization starts in a large part of the region subjected to deformation, and the fraction of dynamically recrystallized volume has reached its maximum in the middle of the blank. In the second reduction, owing to a high temperature staying within the deformation zone combined with considerable magnitudes of deformation in this zone, the dynamic recrystallization process covered a larger part of the plastic zone volume, which resulted in an

increase in the dynamically recrystallized volume fraction up to 70%. The distribution of mean grain size on the specimen cross-sectional surface is non-uniform. The smallest grain size, 24.0 μm, was obtained for the middle blank region. On the deformed metal-anvils contact surface, much larger mean grain sizes (44.0 μm) were obtained.

The distribution of the dynamically recrystallized volume fraction and the distribution of mean grain size on the cross-sectional surface of Ti-6Al-4V alloy specimens after the cogging process (after the second reduction) in radial-rhombic anvils with an impression angle of 135°/135° are represented in Figure 7. The tool under consideration produced a microstructure that was largely recrystallized and homogenous in the most part of the specimen cross-section. The dynamic recrystallization commences in a large part of the region undergoing the greatest deformation, located in the axial zone of the blank, where the fraction of dynamically recrystallized volume has reached its maximum of 88.6% (for a reduction of 0.70). For the side blank zones and for the region located under the anvil corner radii, the dynamically recrystallized volume fraction assumed smaller values, ranging from 31.4% to 42.9%, with higher values concerning the side blank zones. The distribution of mean grain size on the specimen cross-sectional surface is more uniform compared to that for the flat anvils. The intensive forge-out of the blank axial zone in 135°/135° angle radial-rhombic anvils favors the formation of a fine-grained structure in this region, whose grain size
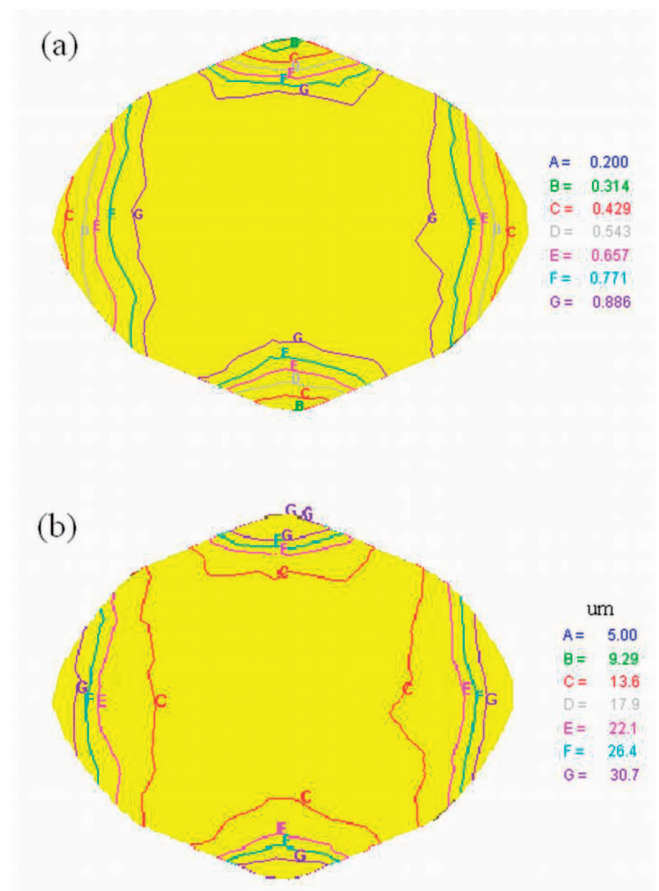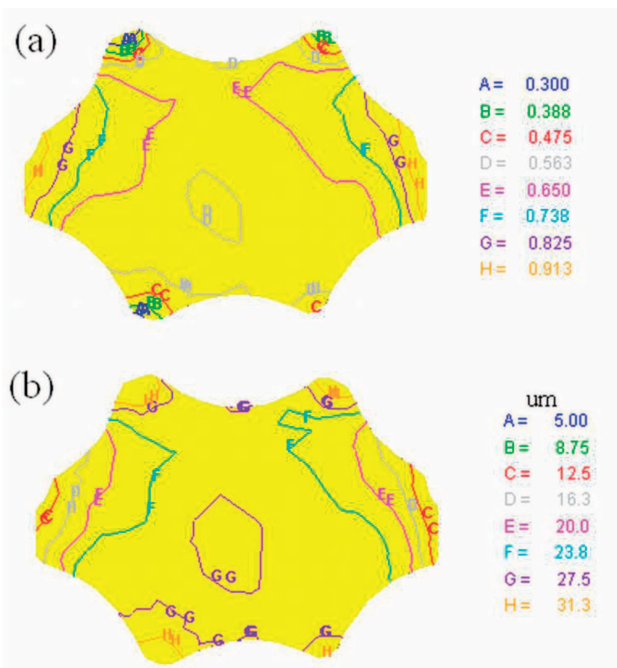

Fig. 7. Distribution of the dynamically recrystallized volume fraction (a) and mean grain size (b) on the specimen cross-sectional surface after cogging process in radial-rhombic anvils with an impression angle of $\alpha = 135°/135°$. True strain $\varepsilon_h = 0.70$

amounted to 13.6 μm (for a reduction of 0.70). For the side blank zones and for the area located under the anvil corner radii, the mean grain size was larger, amounting to 30.7 μm.

The distribution of the dynamically recrystallized volume fraction and the distribution of mean grain size on the cross-sectional surface of Ti-6Al-4V alloy specimens after the cogging process (after the second reduction) in special tri-radial anvils are represented in Figure 8. The tool under consideration caused a microstructure to be obtained, which was largely recrystallized and homogenous in the most part of the blank cross-section. The dynamic recrystallization started in a large part of the region subjected to the greatest deformation located under the convex anvil surfaces, where the fraction of dynamically recrystallized volume had reached its maximum of 65 - 82.5%, with higher values concerning the zone of the direct contact between the deformed material and the anvils.

For the middle region of the blank, the fraction of dynamically recrystallized volume took on smaller values, amounting to 56%. The distribution of mean grain size on the specimen cross-sectional surface is more uniform compared to that for the flat anvils and the 135°/135° angle radial-rhombic anvils. The smallest grain size, 16 - 20 μm, was obtained for the area located under the convex anvil surface. For the middle part of the blank, the mean grain size was larger, amounting to 27.5 μm.

effect was achieved in the special tri-radial anvils. For the flat anvils, these were the zones of hampered deformation, where, due to small deformations, the grain sizes little changed (d = 44 μm). Moreover, the highest non-uniformity of the mean grain size distribution, with an unfavorable stress state in the side blank zones, was obtained in the flat anvils. The comparative analysis confirmed the advisability of using special tri-radial anvils for rough forging of two-phase titanium alloys. The convex shape of the anvil working surfaces enabled relatively high and uniform effective strain values to be achieved in the deformation zone volume under favorable stress state conditions. Introducing special tri-radial anvils in the initial phase of cogging, combined with subsequent deformation in 135°/135° angle radial-rhombic anvils, will make it possible to achieve uniform plastic working within the bulk of the titanium blank and to obtain an homogeneous and fine-grained microstructure.

The experimental confirmation of the results of the numerical examination of effective strain distribution in the 135°/135° radial-rhombic anvils is illustrated in Fig. 9. The strain state has been determined using the coordination grid method. Comparisons between the experimental and simulated results after the cogging process in special tri-radial anvils are presented in Fig. 10 (the temperature of the longitudinal section – Fig. 10a, the average grain sizes in the centre of the specimens deformed at a different true strain – Fig. 10b.). The simulation results predict well the experimental measurements.
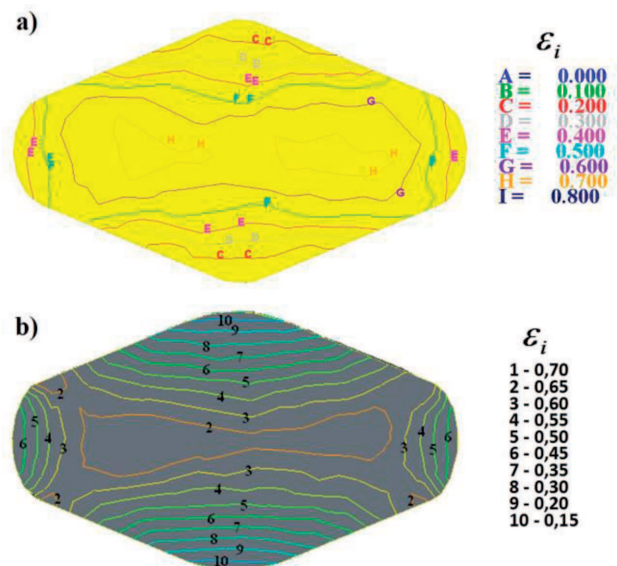

Fig. 8. Distribution of the dynamically recrystallized volume fraction (a) and mean grain size (b) on the specimen cross-sectional surface after cogging process in special tri-radial anvils. True strain ε_h = 0.70

Fig. 9. Comparison of the theoretical (a) and experimental (b) effective strain (ε_i) distribution on the cross-sectional surfaces of Ti-6Al-4V alloy specimens deformed in radial-rhombic anvils with an impression angle of α =135°/135°. Relative feed l_w = 0.75, true strain ε_h = 0.35

A comparative analysis found that the greatest grain refinement effect in the axial blank zone during forging the Ti-6Al-4V alloy was achieved in the 135°/135° angle radial-rhombic anvils (d =13.6 μm) and, at the same time, with the increase in reduction the effective strain increased and a significant grain size reduction followed. In the deformed metal-tool contact zones, the greatest grain size refinement
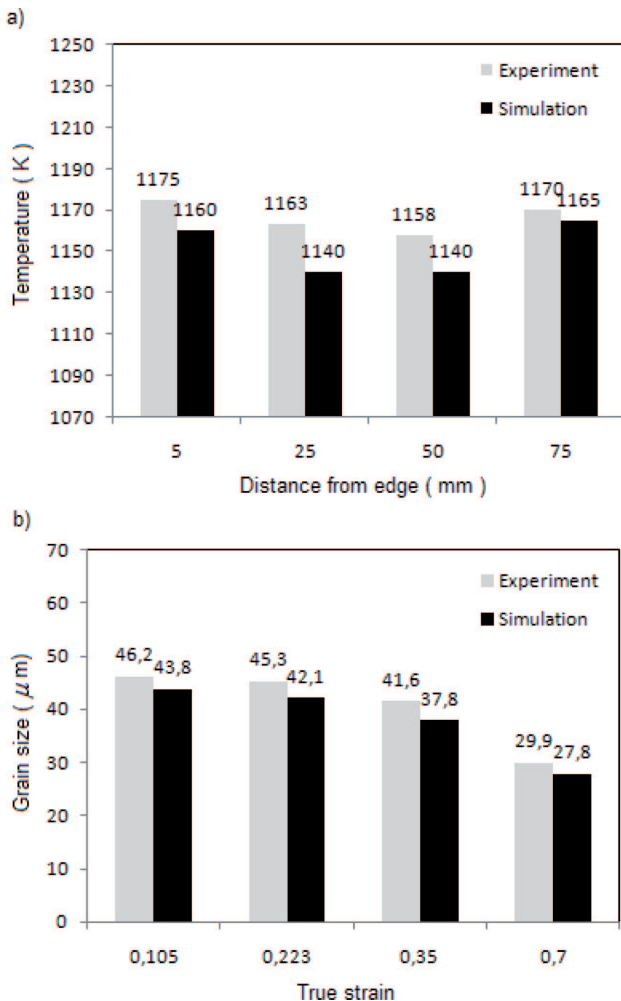
a)

b)

Fig. 10. Comparisons between the experimental and simulated results after cogging process in special tri-radial anvils: (a) temperature of the longitudinal section ($l_w = 0.75$; $\varepsilon_h = 0.70$), (b) average grain sizes in the centre of the specimens deformed at different true strain

5. Conclusions

The investigation carried out has determined the local values describing the strain state and the stress state during cogging of the Ti-6Al-4V alloy in both flat and shape anvils. Through the selection of the appropriate shape and geometry of the anvil working surface and the rational engineering parameters it will be possible to significantly influence: the location of maximal effective strain values, the magnitude of strain distribution non-uniformity and the reduction of the tensile stress share of the deformation zone. Introducing a special tri-radial anvils in the initial phase of cogging, combined with subsequent deformation in 135°/135° angle radial-rhombic anvils, will make it possible to achieve effective strain fields close to the uniform field. The consider-

able non-dilatational (redundant) strains that occur during the process of cogging in shape anvils substantially influence the shape and size of the grains, which can be changed in a broad range, thus influencing the properties of the forging.

Introducing system forging results in significant changes to the metal flow kinematics. The use of different anvils in the process of cogging of two-phase titanium alloys creates possibilities for making use of a combination of their individual advantages. The different location of extreme effective strain values and their mutual movement during the multi-stage cogging process favor uniform and adequate forging out of the metal and obtaining an optimal microstructure. The final forging operations can be carried out in flat anvils.

REFERENCES

[1] R. Filip, K. Kubiak, W. Ziaja, J. Sieniawski, The effect of microstructure on the mechanical properties of two-phase titanium alloys, Journal of Materials Processing Technology **133**, 84-89 (2003).
[2] E.N. Cumacenko, B. Kukuryk, Analysis of superplastic forming of the titanium hemispherical shape, Rudy i Metale Nieżelazne **52**, 677-682 (2007).
[3] N.K. Park, J.T. Yeom, Y.S. Na, Characterization of deformation stability in hot forging of conventional Ti-6Al-4V using processing maps, Journal of Materials Processing Technology **130-131**, 540-546 (2002).
[4] S.K. Choi, M.S. Chun, C.J. Van-Tyne, Y.H. Moon, Optimization of open die forging of round shapes using FEM analysis, Journal of Materials Processing Technology **172**, 88-95 (2006).
[5] F. Warchowicka, M. Stockinger, H.P. Degischer, Quantitative analysis of the microstructure of near β titanium alloy during compression tests, Journal of Materials Processing Technology **177**, 473-477 (2006).
[6] R. Srinivasan, M. Balathandayuthapani, W. Yan, Temperature changes and loads during hot-die forging of a gamma titanium – aluminide alloy, Journal of Materials Processing Technology **160**, 321-334 (2005).
[7] B. Kukuryk, The influence of thermomechanical parameters on the forging process of titanium alloys, Rudy i Metale Nieżelazne **52**, 901-906 (2007).
[8] M. Mulyadi, M.A. Rist, L. Edwards, J.W. Brooks, Parameter optimisation in constitutive equations for hot forging, Journal of Materials Processing Technology **177**, 311-314 (2006).
[9] J. Fluhrer, Deform 3D User's Manual Version 6.0, Scientific Forming Technologies Corporation, Columbus, OH (2006).
[10] M. Schikorra, L. Donati, L. Tomesani, A.E. Tekkaya, Microstructure analysis of aluminium extrusion: Prediction of microstructure on AA6060 alloy, Journal of Materials Processing Technology **201**, 156-162 (2008).
[11] F.S. Du, M.T. Wang, X.T. Li, Research on deformation and microstructure evolution during forging of large – scale parts, Journal of Materials Processing Technology **187-188**, 591-594 (2007).